


Screening Xanthene Dyes for Visible Light-Driven Nicotinamide Adenine Dinucleotide Regeneration and Photoenzymatic Synthesis

Sahng Ha Lee,^a Dong Heon Nam,^a and Chan Beum Park^{a,*}

^a Department of Materials Science and Engineering, Institutes for the BioCentury (KIB) and the NanoCentury (KINC), Korea Advanced Institute of Science and Technology (KAIST), 335 Science Road, Daejeon 305-701, Republic of Korea
Fax: (+82)-42-350-3310; e-mail: parkcb@kaist.ac.kr

Received: August 3, 2009; Published online: October 22, 2009

 Supporting information for this article is available on the WWW under <http://dx.doi.org/10.1002/adsc.200900547>.

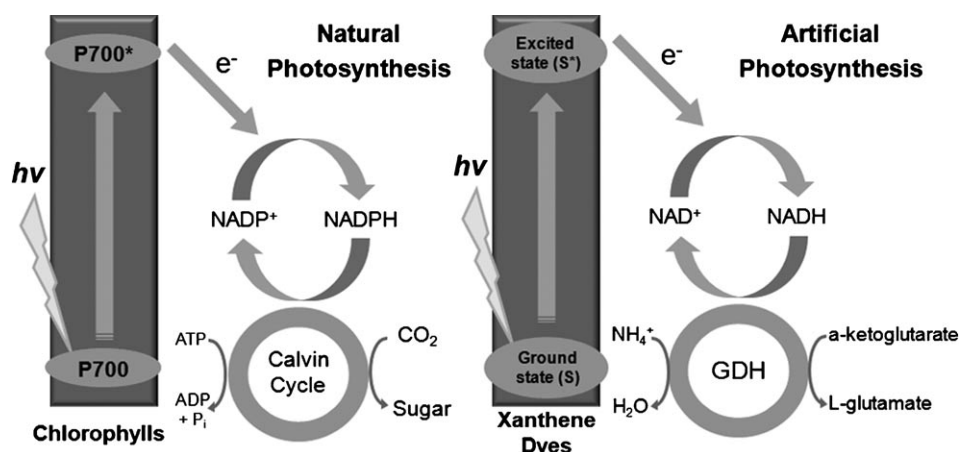
Abstract: Regeneration of the nicotinamide cofactor is a critical issue in biocatalysis. Herein we have screened xanthene dyes for a highly efficient, visible light-driven photochemical regeneration of cofactors and enzymatic synthesis. Superior catalytic performance was observed with several xanthene dyes such as phloxine B, erythrosine B, eosin Y, and rose bengal. We found that the photo- and electrochemical properties of the xanthene dyes were affected by the halogen atom substitution, which is a key factor in the efficient light-induced electron transfer from the donor molecule to the catalytic mediator.

Keywords: artificial photosynthesis; cofactor regeneration; homogeneous catalysis; photoenzymatic synthesis; xanthene dyes

Oxidoreductases can catalyze difficult redox reactions that conventional chemical catalysts are unable to catalyze.^[1] Despite the capability of oxidoreductases to catalyze complex reactions, they require a stoichiometric amount of cofactors that have two contrary states (i.e., oxidized *vs.* reduced). Numerous efforts have been made for the *in situ* regeneration of cofactors, such as nicotinamide adenine dinucleotide (NADH), from its consumed counterparts towards the practical application of oxidoreductases in industrial biosynthesis.^[2,3] While conventional cofactor regeneration methods, such as the use of second enzymes or chemical electrodes, have such drawbacks as catalyst instability, low specific activity, and limited applications,^[4] the photochemical route to cofactor regeneration is at its infancy, providing an opportunity to utilize clean and abundant solar energy.^[5,6] A few studies report on the photochemical regeneration of

cofactors by using heterogeneous semiconductor powders^[7–10] or soluble organic/organometallic materials as a photosensitizer.^[11–13] However, photochemical approaches suffer from extremely low turnover frequency and synthetic yield because they lack an efficient light-harvesting component.^[8,9]

In nature, photosynthesis is achieved through photosystems with natural organic dyes, such as chlorophylls, used to collect solar energy. As shown in Scheme 1, cofactors are regenerated into a reduced form by the transfer of light-excited electrons, for their use in the Calvin cycle.^[14] While natural photosystems provide hints about the design of efficient solar energy utilization in connection to biocatalysis, the rate of natural photosynthesis is too low to be directly used in synthetic biocatalysis. Thus, it has been a long-standing challenge to design an artificial photosynthetic system that can work efficiently in the visible-light range.^[15] On the other hand, with regard to solar energy utilization, many efforts have been devoted to the development of an efficient light-harvesting system that can convert solar energy into electrical or chemical energy through a man-made photovoltaic assembly.^[16] Among photovoltaic sensitizers, xanthene dyes are known to possess a good photochemical redox property, which enables their applications to dye-sensitized solar cells (DSSCs) and photocatalytic hydrogen evolution.^[17,18] They undergo an internal singlet-triplet transition by light absorption, and the photo-excited triplet electrons of xanthenes can then be transferred to catalytic reagents^[19] and semiconductor materials.^[20] Visible light-active fluorescence of xanthene dyes (e.g., fluorescein, rhodamine) is being widely used as an imaging marker for living cells and as a tracer for biomolecules.^[21] In spite of their high potential for use in photochemical applications, xanthene dyes had rarely been applied to photosynthesis.



Scheme 1. An illustrative description of natural photosynthesis (*left*) in comparison with artificial photosynthesis (*right*). In both systems, photosynthesis is achieved through photosystems with organic dyes collecting solar energy, followed by the regeneration of nicotinamide cofactors in a reduced form by the transfer of light-excited electrons for their use in enzymatic synthesis.

Recently we reported that eosin Y, one of xanthene dyes, works as an efficient light harvester for artificial photosynthesis.^[22] Inspired by that work, herein we have screened xanthene dyes for the visible light-driven, non-enzymatic regeneration of NADH, coupled with a redox reaction catalyzed by L-glutamate dehydrogenase (GDH). In the artificial photosynthetic system, which is illustratively described in Scheme 1, we studied the possibility of using xanthene dyes as a photosensitizing organic dye in place of a natural pigment (e.g., chlorophylls). As a hydride-transfer mediator during the cofactor regeneration process, we used a rhodium-based organometallic compound, **M** ($[\text{Cp}^*\text{Rh}(\text{bpy})\text{H}_2\text{O}]^{2+}$), instead of ferredoxin-NADP⁺ reductase used in natural photosynthetic processes. **M** had been recognized as a versatile tool for the regeneration of NADH in an “enzymatically-active” form with high selectivity.^[23–26]

We evaluated ten different types of xanthene dyes, the structures of which are listed in Figure 1, to investigate their capability for photochemical NADH regeneration during dye-sensitized artificial photosynthesis. According to our results, the ability of each xanthene dye to drive photochemical NADH regeneration was significantly affected by a slight change in its chemical structure. As shown in Figure 2, six xanthene dyes, including fluorescein and its halogen-substituted derivatives (i.e., eosin Y, erythrosine B, merbromin, phloxine B, and rose bengal), were capable of inducing NADH photo-regeneration, while the other four dyes did not exhibit any activity. NADH generation did not occur at all without the irradiation of visible light ($\lambda \geq 420$ nm). After the rapid reduction of NAD⁺ to a maximum conversion within 20 min by light irradiation, a gradual oxidation of the regenerated NADH was observed for merbromin, phloxine B, and rose bengal.

NADH has different isomeric forms, only one of which can be utilized for enzymatic synthesis reaction.^[6] Thus, for the application of photochemically regenerated NADH to artificial photosynthesis, the cofactor should be in an enzymatically active form. In this work, we coupled the photochemical NADH regeneration with an L-glutamate synthesis reaction from α -ketoglutarate, catalyzed by GDH. As shown in Figure 3 and Figure S1 in the Supporting Information, eosin Y, erythrosine B, merbromin, phloxine B, and rose bengal showed superior performances in terms of synthetic yield and reaction rate in the photoenzymatic synthesis of L-glutamate. The highest turnover frequency (TOF) of a photosensitizer was observed with phloxine B (1537.3 h^{-1}). A similar level of TOF was observed for other halogen-substituted dyes, like eosin Y (1177.5 h^{-1}), erythrosine B (1144.8 h^{-1}), and rose bengal (1270.8 h^{-1}), which are at least two-orders higher than the results reported previously with organic photosensitizers such as PEG-chlorophyllide^[13] and $\text{Ru}(\text{bpy})_3$.^[12] In addition, we obtained high conversion yields and turnover numbers of NAD⁺ from the xanthene dye-sensitized photoenzymatic reactions (Figure S1, Supporting Information).

We studied the changes of absorbance spectra of the six dyes that were active for NADH photoregeneration in the presence of **M**, the organometallic mediator. According to our results, with the addition of **M**, their absorbance spectra exhibited red-shifted onsets and peaks with the addition of **M** (Figure S2, Supporting Information). There were negligible changes in absorbance spectra for the rhodamine series (rhodamine B, rhodamine 6G, and sulforhodamine B), which were unable to drive NADH regeneration. Since xanthene dye's fluorescence is known to originate from the excitation of internal elec-

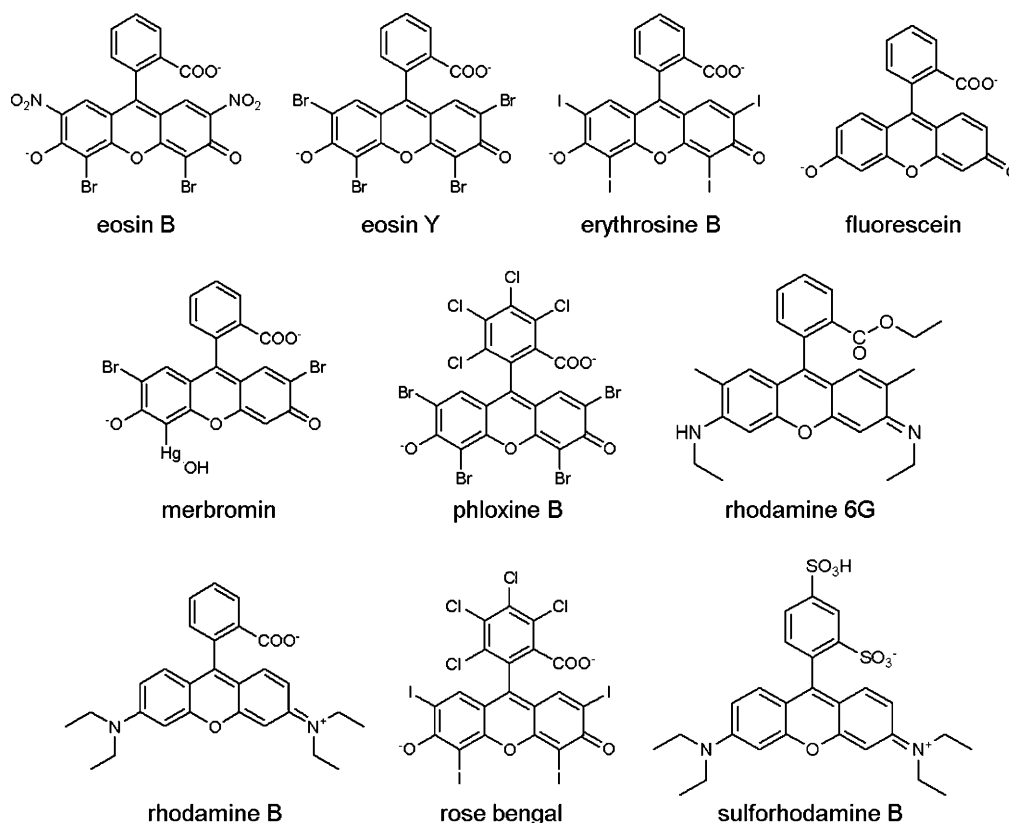


Figure 1. Molecular structures of xanthene dyes studied in this work.

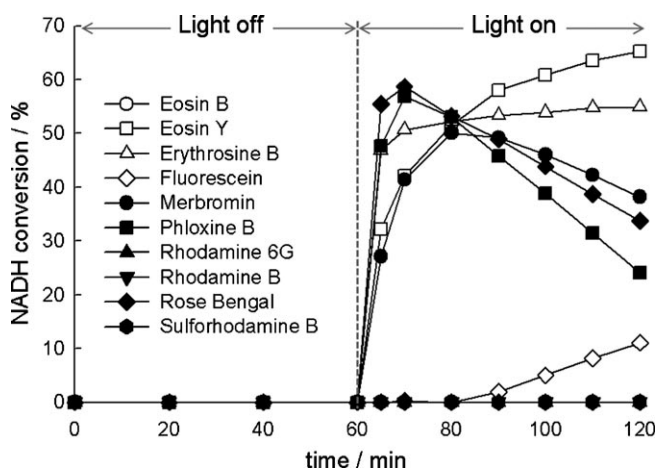


Figure 2. NADH regeneration from NAD^+ (1 mM) by the photosensitization of xanthenes (5 μM). After incubation under a dark stage for 1 hour, visible-light ($\lambda \geq 420 \text{ nm}$) was irradiated to the reactor.

trons,^[27] we suggest that the fluorescent energy transfer reaction occurs between xanthene dye and **M**. In order to study the donor-acceptor relationship between each dye and **M**, we studied their fluorescence behaviors through the Stern–Volmer relationship^[28] as a function of the concentration of **M** ($[\text{M}]$) (i.e., $F_0/F = 1 + K_{\text{SV}} [\text{M}]$, where F_0 and F are fluorescence in-

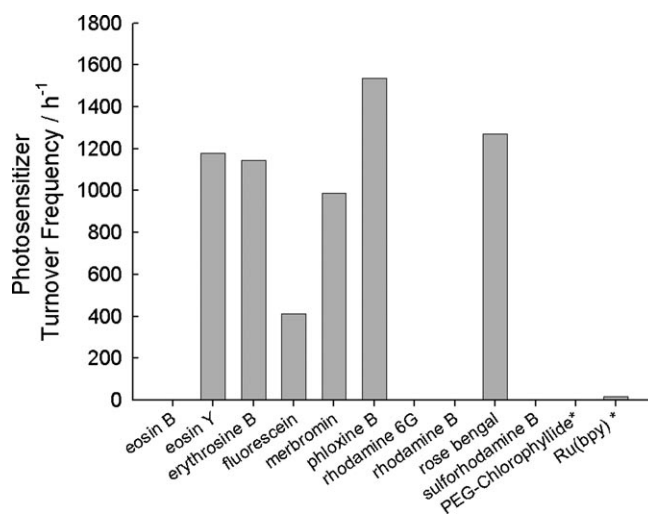


Figure 3. The photosensitizer turnover frequency of xanthene dyes measured for the enzymatic photosynthesis of L-glutamate, in comparison with previous reports* [PEG-chlorophyllide^[13] and $\text{Ru}(\text{bpy})_3$ ^[12]].

tensities in the absence and presence of **M**, respectively). Shown in Figure 4a are the Stern–Volmer plots, from which the Stern–Volmer constants (K_{SV}) were evaluated for each dye (Figure 4b). With increasing $[\text{M}]$, we observed a drastic quenching of

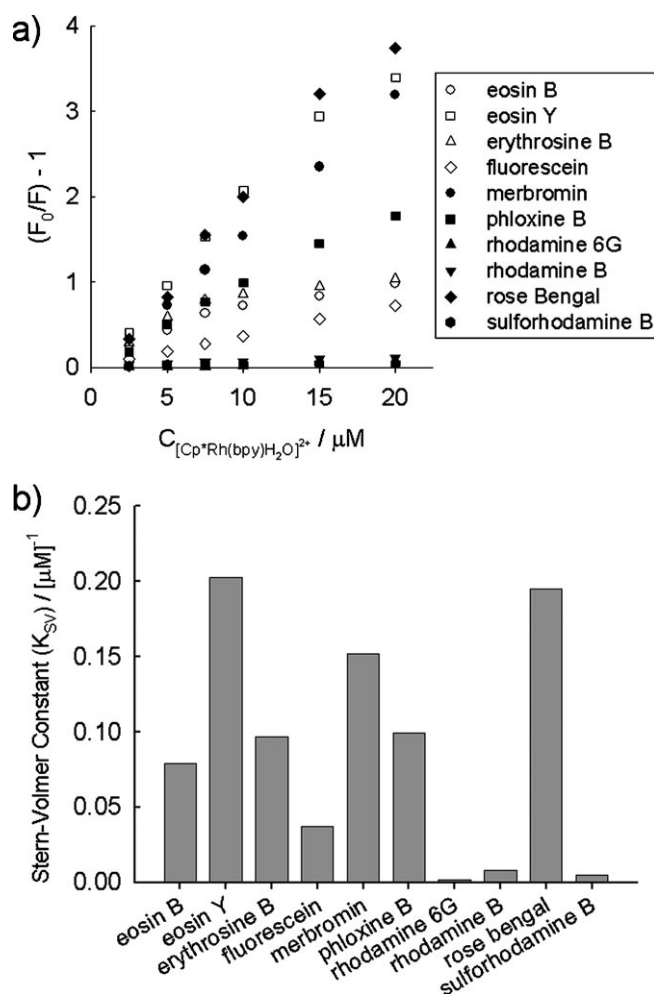


Figure 4. Stern–Volmer relationship between xanthene dyes (5 μM) and M in various concentrations. a) Stern–Volmer plot and b) Stern–Volmer constant (K_{SV} , determined from the slope of each plot in the Stern–Volmer plot). Drastic quenching of fluorescence with high K_{SV} was observed from dyes that were active for NADH photoregeneration, except for eosin B.

fluorescence (i.e., high value of K_{SV}) for most dyes that were active for NADH photoregeneration. Eosin B was an exceptional case, since its optical properties (i.e., absorbance and fluorescence) changed in the presence of $[M]$, but did not exhibit any activity for NADH regeneration. We analyzed the electrochemical property of eosin B in comparison with M by using a linear sweep voltammetry (LSV) measurement (Figure S3, Supporting Information). The voltammetric result indicates that the reduction potential of eosin B (−0.604), which can be interpreted as its LUMO,^[29] is lower than the potential required to reduce M (−0.719), unlike other dyes that were active for NADH regeneration. This result indicates that the excited electrons of eosin B have insufficient energy to reduce M , thus failing in the regeneration of NADH.

We further investigated the effect of halogen atom substitution in xanthene dyes on the performance of NADH regeneration. In particular, we focused on five dyes with similar structures: fluorescein, eosin Y, erythrosine B, phloxine B, and rose bengal, in which the 2,4,5,7-hydrogen atoms of fluorescein are substituted by Br (eosin Y) or I (erythrosine B), along with an additional substitution of the 3',4',5',6'-hydrogen atoms by Cl (phloxine B and rose bengal). The activities of these dyes for NADH photoregeneration increased in the order of heavy halogen atom substitution: fluorescein < eosin Y < erythrosine B < phloxine B < rose bengal. According to the literature,^[27] heavy atom substitution can enhance the transition state of the aromatic molecule's singlet-triplet state by increasing the spin-orbit mixing. As the substituted atom becomes heavier, the dye's electronegativity decreases, enhancing the electron-donation capability in the order of $H < Cl < Br < I$.^[30] Furthermore, the decrease in the dye's electronegativity, due to the heavy atom substitution, affects its electron-accepting ability, making the dye an acceptor in the reverse order (i.e., $I < Br < Cl < H$).^[31] We further studied the effect of halogen atom substitution on the electrochemical property of the dyes by using a linear sweep voltammetry (LSV) measurement (Figure S3, Supporting Information). We observed that the reduction potential of each dye increased in the order of decreasing electronegativity ($H < Cl < Br < I$), which is most likely due to the increasing electron-accepting ability of the dye in the ground state.

In summary, we found that xanthene dyes can work as a promising visible light-harvesting catalytic component for the highly efficient photoregeneration of NADH and enzymatic synthesis. The turnover rate of the cofactor significantly enhances in the visible light-driven photocatalytic reaction, sensitized by xanthene dyes. A donor-acceptor relationship was observed between the organometallic mediator and xanthene dyes, excepting the rhodamine series. Photo- and electrochemical properties of xanthene dyes were affected by the halogen atom substitution, which is a key factor in the efficient light-induced electron transfer from the donor molecule to the catalytic mediator. We anticipate that our finding about the superior performance of xanthene dyes for photoenzymatic synthesis will provide a foundation for developing efficient artificial photosynthetic systems driven by solar light.

Experimental Section

Materials

All chemicals, including xanthene dyes, triethanolamine (TEOA), and NAD^+ , were purchased from Sigma–Aldrich

(St. Louis, MO) in the purity over reagent grade and were used without further purification. Stock solutions of xanthene dyes (1 mM) were prepared by dissolving the dyes in deionized water for further experiments.

Synthesis of [Cp*Rh(bpy)Cl]Cl

The hydridorhodium complex, **M**, was synthesized according to the literature.^[23–25] A mixture of RhCl₃·3H₂O (200 mg) and hexamethyl-Dewar-benzene (HMDB) in methanol was refluxed at 65°C under nitrogen for 15 h. At room temperature, the solvent was then removed under vacuum, and the residue was washed with ether to remove excess the hexamethylbenzene. The remaining oily red crystals were extracted with chloroform and the solution was dried over anhydrous magnesium sulphate. After evaporation under reduced pressure, the residue was recrystallized from chloroform-benzene. The product was dissolved in methanol and with the addition of two equivalents of 2,2'-bipyridine, the suspension cleared up almost immediately to afford a yellowish solution. [Cp*Rh(bpy)Cl]Cl was then precipitated by the addition of diethyl ether and the final compound was further confirmed by an NMR spectroscopic analysis (300 MHz, Bruker, Germany); ¹H NMR (300 MHz, CDCl₃): δ = 9.11 (d, 2H, H-3,3'), 8.84 (d, 2H, H-6,6'), 8.27 (t, 2H, H-5,5'), 7.81 (t, 2H, H-4,4'), 1.75 (s, 15H, Cp*).

Photochemical Reaction

The photochemical regeneration of NADH was performed in a quartz reactor under an argon atmosphere at room temperature. A 450 Watt Xe-lamp (Oriel Co.), equipped with a 420 nm cut-off filter was used as light source. The dye-sensitized photoregeneration of NADH was carried out by light illumination to a quartz reactor containing 1 mM NAD⁺, 0.25 mM **M**, 15 w/v% TEOA, and 100 mM phosphate buffer (pH 7.4) with xanthenes (5 μM). For the enzymatic photosynthesis of L-glutamate, we conducted the reaction with NAD⁺ (50 μM), xanthenes (20 μM), **M** (250 μM), α-ketoglutarate (10 mM), ammonium sulphate (200 mM) and GDH (40 U), based on a 0.1 M phosphate buffer (pH 7.4) containing 15 w/v% TEOA.

Analysis

Spectrophotometric and spectrofluorometric experiments were performed with the BioSpec-mini and RF-5301PC (Shimadzu Co., Japan), respectively. In both measurements, 5 μM of xanthene dyes were used with various concentrations of **M**. The fluorescence spectra were obtained with an excitation wavelength of 350 nm. Voltammetric experiments were performed with a single cell compartment configured with a 3-electrode system: a glassy carbon or Au disk (working diameter 2 mm), a platinum wire (counter), and an Ag/AgCl_{saturated KCl} (reference, 0.197 V versus normal hydrogen electrode) connected to a potentiostat/galvanostat (EG&G, model 263 A). **M** (0.5 mM) and xanthene dyes (1 mM) were prepared in a phosphate buffer (100 mM) at pH 7.0. The concentration of NADH was measured spectrophotometrically through the analysis of its absorbance at 340 nm.

Acknowledgements

This work was supported by grants from Korea Science and Engineering Foundation (KOSEF), National Research Laboratory (ROA-2008-000-20041-0) and Engineering Research Center (R11-2008-058-03003-0) Programs. This research was also partially supported by the High Risk High Return Project (HRHRP) from the office of KAIST, Republic of Korea.

References

- [1] H. Zhao, W. A. van der Donk, *Curr. Opin. Biotechnol.* **2003**, *14*, 1–7.
- [2] J. B. van Beilen, W. A. Duetz, A. Schmid, B. Witholt, *Trends Biotechnol.* **2003**, *21*, 170–177.
- [3] R. Devaux-Basseguy, A. Bergel, M. Comtat, *Enzyme Microb. Technol.* **1997**, *20*, 248–258.
- [4] F. Hollmann, K. Hofstetter, A. Schmid, *Trends Biotechnol.* **2006**, *24*, 163–171.
- [5] W. A. van der Donk, H. Zhao, *Curr. Opin. Biotechnol.* **2003**, *14*, 421–426.
- [6] F. Hollmann, A. Schmid, *Biocatal. Biotransform.* **2004**, *22*, 63–88.
- [7] Z. Goren, N. Lapidot, I. Willner, *J. Mol. Catal.* **1988**, *47*, 21–32.
- [8] Q. Shi, D. Yang, Z. Jiang, J. Li, *J. Mol. Catal. B: Enzym.* **2006**, *43*, 44–48.
- [9] Z. Jiang, C. Lü, H. Wu, *Ind. Eng. Chem. Res.* **2005**, *44*, 4165–4170.
- [10] C. B. Park, S. H. Lee, E. Subramaniam, B. B. Kale, S. M. Lee, J. O. Baeg, *Chem. Commun.* **2008**, 5423–5425.
- [11] R. Wienkamp, E. Steckhan, *Angew. Chem.* **1983**, *95*, 508–509; *Angew. Chem. Int. Ed. Engl.* **1983**, *22*, 497–498.
- [12] D. Mandler, I. Willner, *J. Chem. Soc. Perkin Trans. 2* **1986**, 805–811.
- [13] H. Asada, T. Itoh, Y. Kodera, A. Matsushima, M. Hiroto, H. Nishimura, Y. Inada, *Biotechnol. Bioeng.* **2001**, *76*, 86–90.
- [14] J. H. Alstrum-Acevedo, M. K. Brennaman, T. J. Meyer, *Inorg. Chem.* **2005**, *44*, 6802–6827.
- [15] D. Gust, T. A. Moore, A. L. Moore, *Acc. Chem. Res.* **2001**, *34*, 40–48.
- [16] N. S. Lewis, D. G. Nocera, *Proc. Natl. Acad. Sci. USA* **2006**, *103*, 15729–15735.
- [17] G. Ramakrishna, H. N. Ghosh, *J. Phys. Chem. B* **2001**, *105*, 7000–7008.
- [18] S. Pelet, M. Grätzel, J. E. Moser, *J. Phys. Chem. B* **2003**, *107*, 3215–3224.
- [19] S. D. M. Islam, T. Konishi, M. Fujitsuka, O. Ito, Y. Nakamura, Y. Usui, *Photochem. Photobiol.* **2000**, *71*, 675–680.
- [20] Z. Jin, X. Zhang, G. Lu, S. Li, *J. Mol. Catal. A: Chem.* **2006**, *259*, 275–280.
- [21] J. Shi, X. Zhang, D. C. Neckers, *J. Org. Chem.* **1992**, *57*, 4418–4421.
- [22] S. H. Lee, D. H. Nam, J. H. Kim, C. B. Park, *ChemBioChem* **2009**, *10*, 1621–1624.
- [23] E. Steckhan, S. Herrmann, R. Ruppert, E. Dietz, M. Frede, E. Spika, *Organometallics* **1991**, *10*, 1568–1577.

- [24] H. C. Lo, C. Leiva, O. Buriez, J. B. Kerr, M. M. Olmstead, R. H. Fish, *Inorg. Chem.* **2001**, *40*, 6705–6716.
- [25] F. Hollmann, B. Witholt, A. Schmid, *J. Mol. Catal. B: Enzym.* **2003**, *19–20*, 167–176.
- [26] H. K. Song, S. H. Lee, K. Won, J. H. Park, J. K. Kim, H. Lee, S. J. Moon, D. K. Kim, C. B. Park, *Angew. Chem.* **2008**, *120*, 1773–1776; *Angew. Chem. Int. Ed.* **2008**, *47*, 1749–1752.
- [27] N. B. Joshi, P. Gangola, D. D. Pant, *J. Lumin.* **1979**, *21*, 111–118.
- [28] J. J. McCullough, W. K. MacInnis, C. J. L. Lock, R. Fagiani, *J. Am. Chem. Soc.* **1982**, *104*, 4644–4658.
- [29] M. S. Liu, X. Jiang, S. Liu, P. Herguth, A. K. Y. Jen, *Macromolecules* **2002**, *35*, 3532–3538.
- [30] X. F. Zhang, Q. Liu, H. Wang, Z. Fu, F. Zhang, *J. Photochem. Photobiol. A: Chem.* **2008**, *200*, 307–313.
- [31] B. B. Bhowmik, P. Ganguly, *Acta. Mol. Spectros.* **2005**, *61*, 1997–2003.
-